J|A|C|S
ARTICLES
Published on Web 11/23/2004

Crystalline Inclusion Compounds Constructed through Self-Assembly of Isonicotinic Acid and Thiocyanato Coordination Bridges

Ryo Sekiya,*,† Shin-ichi Nishikiori,† and Katsuyuki Ogura‡

Contribution from the Department of Basic Science, Graduate School of Arts and Sciences, The University of Tokyo, 3-8-1 Komaba, Meguroku, Tokyo 153-8902, Japan, and Department of Materials Technology, Faculty of Engineering, Chiba University, 1-33 Yayoicho, Inageku, Chiba 263-8522, Japan

Received June 22, 2004; E-mail: csekiya@mail.ecc.u-tokyo.ac.jp

Abstract: The synthesis, crystal structures, inclusion ability, and structural robustness of novel crystalline inclusion compounds of $[Ni(SCN)_2(isoH)_2]\cdot xG$ (isoH = isonicotinic acid; G = aromatic guest) are described. The inclusion compounds are constructed by stacking identical 2D host layers that consist of SCN^-, isoH, and Ni^{2+} with van der Waals contact separation. In the layer, two types of rectangular cavities (A-type and B-type) are formed, and the guests are included in the former cavity. The inclusion compounds were categorized into four stacking modes according to the difference in the stacking mode of the layers. A systematic investigation of the crystal structures of the 21 inclusion compounds clarified the close relationship between the molecular structure of the guest and the resultant stacking mode of the layers.

Introduction

The molecular recognition/inclusion event of organic and metal−organic coordination hosts has been the focus of research interest since the discovery of the first inclusion compound at the middle of the 19th century.[1] Since then, hundreds of host compounds have been designed and synthesized, and their inclusion abilities and applications to functional materials have been studied in great detail. The discovery of host compounds such as urea, *n*-cyclodextrins ($n = \alpha$, β, and γ), calix[*i*]arenes, crown ethers, wheel-and-axel-type inclusion compounds, deoxycholic acid, Werner-type inclusion compounds, and Hofmann-type inclusion compounds has played an important role in the development of inclusion chemistry and related material science.[2,3] This molecular recognition/inclusion event has been investigated mainly in solution and crystalline phases. Our current interest is crystalline inclusion compounds, in particular those constructed through self-assembly of transition metal ions and molecular building blocks because of their potential applications to reaction chamber,[4,5] gas storage devices,[6−9] and catalysis,[10−12] and their physical properties which cannot be generated by discrete molecules,[13−17] as well as selective inclusion of specific guest molecules.[18−31]

One of the current topics of modern inclusion chemistry is the question of how to construct a host framework with a

† The University of Tokyo.
‡ Chiba University.

(1) Lehn, J.-M. *Science* **2002**, *295*, 2400−2402.
(2) Atwood, J. L., Davies, J. E. D., MacNicol, D. D., Eds. *Inclusion Compounds*; Academic Press Inc.: London, 1984.
(3) Atwood, J. L., Davies, J. E. D., MacNicol, D. D., Vögtle, F., Lehn, J.-M., Eds. *Comprehensive Supramolecular Chemistry*; Pergamon: Oxford, 1996.
(4) Toda, F. *Acc. Chem. Res.* **1995**, *28*, 480−486.
(5) Matsumoto, A.; Odani, T.; Chikada, M.; Sada, K.; Miyata, M. *J. Am. Chem. Soc.* **1999**, *121*, 11122−11129.
(6) Noro, S.; Kitagawa, S.; Kondo, M.; Seki, K. *Angew. Chem., Int. Ed.* **2000**, *39*, 2082−2084.
(7) Eddaoudi, M.; Li, H.; Yaghi, O. M. *J. Am. Chem. Soc.* **2000**, *122*, 1391−1397.
(8) Eddaoudi, M.; Kim, J.; Rosi, N.; Vodak, D.; Wachter, J.; O'Keeffe, M.; Yaghi, O. M. *Science* **2002**, *295*, 469−472.
(9) Rosi, N. L.; Eckert, J.; Eddaoudi, M.; Vodak, D. T.; Kim, J.; O'Keeffe, M.; Yaghi, O. M. *Science* **2003**, *300*, 1127−1129.
(10) Fujita, M.; Kwon, Y.; Washizu, S.; Ogura, K. *J. Am. Chem. Soc.* **1994**, *116*, 1151−1152.
(11) Seo, J. S.; Whang, D.; Lee, H.; Jun, S. I.; Oh, J.; Jeon, Y.; Kim, K. *Nature* **2000**, *404*, 982−986.
(12) Li, H.; Davis, C. E.; Groy, T. L.; Kelley, D. G.; Yaghi, O. M. *J. Am. Chem. Soc.* **1998**, *120*, 2186−2187.
(13) Pauchard, M.; Huber, S.; Méallet Renaut, E.; Mass, H.; Pansu, R.; Calzahaferri, G. *Angew. Chem., Int. Ed.* **2001**, *40*, 2839−2842.
(14) Mass, H.; Calzahaferri, G. A*ngew. Chem., Int. Ed.* **2002**, *41*, 2284−2288.
(15) Calazahaferri, G.; Pauchard, M.; Mass, H.; Huber, S.; Khatyr, A.; Schaafsma, T. *J. Mater. Chem.* **2002**, *12*, 1−13.
(16) Langley, P. J.; Hulliger, J. *Chem. Soc. Rev.* **1999**, *28*, 279−291.
(17) Zhao, R.; Matsumoto, S.; Akazome, M.; Ogura, K. *Tetrahedron* **2002**, *58*, 10233−10241.
(18) Sun, D.; Tham, F. S.; Reed, C. A.; Chaker, L.; Boyd, P. D. W. *J. Am. Chem. Soc.* **2002**, *124*, 6604−6612.
(19) Swift, J. A.; Pivovar, A. M.; Reynolds, A. M.; Ward, M. D. *J. Am. Chem. Soc.* **1998**, *120*, 5887−5894.
(20) Kobayashi, K. *Bull. Chem. Soc. Jpn.* **2003**, *76*, 247−260.
(21) Kemperman, G. J.; Gelder, R.; Dommerholt, F. J.; Paemakers-Franken, P. C.; Klunder, A. J. H.; Zwanenburg, B. *Chem. Eur. J.* **1999**, *5*, 2163−2168.
(22) Sommer, R. D.; Rheingold, A. L.; Goshe, A. J.; Bosnich, B. *J. Am. Chem. Soc.* **2001**, *123*, 3940−3952.
(23) Beketov, K.; Weber, E.; Seidel, J.; Köhnke, K.; Makhkamov, K.; Ibragimov, B. *Chem. Commun.* **1999**, 91−92.
(24) Jetti, R. K. R.; Xue, F.; Mak, T. C. W.; Nangia, A. *J. Chem. Soc., Perkin Trans. 2* **2000**, 1223−1232.
(25) Akazome, M.; Takahashi, T.; Ogura, K. *J. Org. Chem.* **1999**, *64*, 2293−2300.
(26) Hertzsch, T.; Budde, F.; Weber, E.; Hulliger, J.*Angew. Chem., Int. Ed.* **2002**, *41*, 2282−2284.
(27) Thaimattam, R.; Xue, F.; Sarma, J. A. R. P.; Mak, T. C. W.; Desiraju, G. R. *J. Am. Chem. Soc.* **2001**, *123*, 4432−4445.
(28) Biradha, K.; Domasevitch, K. V.; Moulton, B.; Seward, C.; Zaworotko, M. J. *Chem. Commun.* **1999**, 1327−1328.
(29) Ma, B. Q.; Coppens, P. *Chem. Commun.* **2003**, 2290−2291.
(30) Krebs, F. C.; Jørgensen, M. *J. Org. Chem.* **2001**, *66*, 6169−6173.
(31) Endo, K.; Sawaki, T.; Koyanagi, M.; Kobayashi, K.; Masuda, H.; Aoyama, Y. *J. Am. Chem. Soc.* **1995**, *117*, 8341−8352.

Scheme 1. Schematic Representation of the Design Principle for the Crystalline Host of $[Ni(SCN)_2(isoH)_2]_\infty$

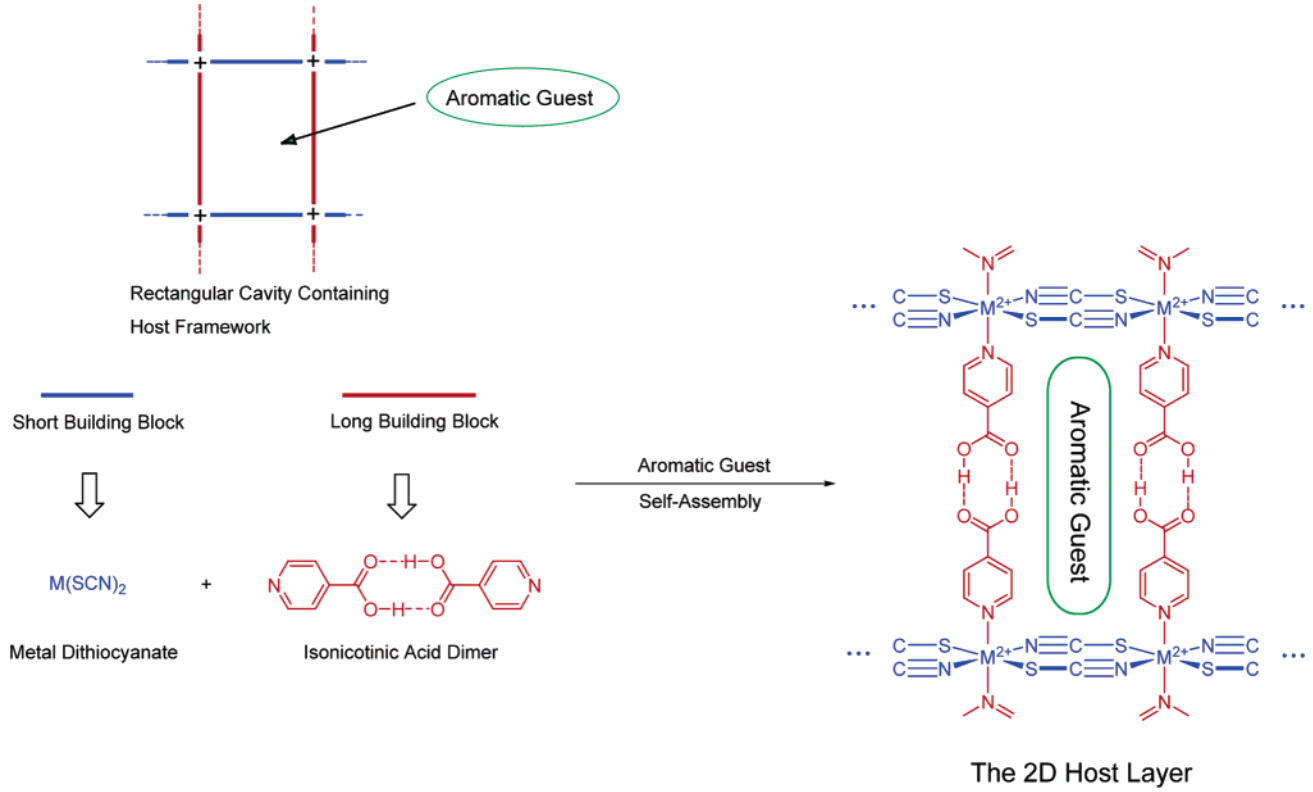

predesigned three-dimensional (3D) structure through appropriate choice of building blocks and control of the process of self-assembly.[6,19,28,29] This is of interest because the nature of a crystalline host is determined to a great extent by the size and shape of an inner cavity or a channel. Therefore, if we can control the 3D structure of the host framework, it should be possible to produce functional materials. Hence, it is natural that many chemists have devoted numerous attempts to achieve this purpose from theoretical and experimental viewpoints.[32,33] Under these circumstances, Desiraju and co-workers have revealed an important role of noncovalent interaction between topologically and chemically complementary functional groups of molecular constituents upon self-assembly through statistical analysis of a vast amount of molecular crystals stored in the Cambridge Structural Database.[33] Despite these investigations, structure prediction of a crystalline inclusion compound is still quite difficult. This is mainly because the crystal structure of a crystalline host is in general quite sensitive to many factors. For example, many metal−organic coordination hosts form different crystal structures as a result of inclusion of different guests,[34] solvent molecules,[35] and counterions.[36]

It is worth noting that inclusion guests reported thus far are usually small organic molecules such as ordinary solvent molecules, benzene, naphthalene, and their analogues, although hundreds of host compounds have been designed and synthesized. This is ascribed to the facile formation of an interpenetrated structure, which is frequently seen in systems where an attempt has been made to construct a large-cavity-containing host framework by using long molecular building blocks.[37,38] Despite this obstacle, inclusion of large organic molecules, in particular those with extended conjugated π-systems or physical properties that can be changed by external stimuli, is of great interest not only from the viewpoint of the fundamental aspect of the molecular recognition/inclusion events but also from that of the applications to optical and electronic materials.[39] Therefore, the design and synthesis of a novel inclusion compound with a predesigned or at least a predictable 3D structure and the ability to include large organic molecules is an important and challenging subject in modern inclusion chemistry.

With these considerations in mind, we report herein the crystal structures, inclusion ability, and structural robustness of crystalline inclusion compounds of $[Ni(SCN)_2(isoH)_2]\cdot xG$ (SCN = thiocyanato ion; isoH = isonicotinic acid; G = guest). Recently, we designed the novel crystalline host of *catena*-bis(*N*-isonicotinic acid)-bis(μ-thiocyanato-*N*,*N*′,*S*,*S*′)nickel(II) with general formula $[Ni(SCN)_2(isoH)_2]\cdot 0.5G$ (G = anthracene[40] and biphenyl[41]). A schematic representation of the design principle for the crystalline host (two-dimensional (2D) host layer) is shown in Scheme 1. The host framework is constructed through self-assembly of isoH, SCN^-, and Ni^{2+}. In the layer, rectangular cavities surrounded by these building blocks are formed. The

(32) Allen, F. H.; Motherwell, W. D. S.; Raithby, P. R.; Shield, G. P.; Taylor, R. *New J. Chem.* **1999**, *23*, 25−34.
(33) Desiraju, G. R. *Angew. Chem., Int. Ed. Engl.* **1995**, *34*, 2311−2327.
(34) Kemperman, G. J.; Gelder, R.; Dommerholt, F. J.; Raemakers-Franken, P. C.; Klunder, A. J. H.; Zwanenburg, B. *Eur. J. Org. Chem.* **2001**, 3641−3650.
(35) Iwamoto, T.; Nishikiori, S.; Kitagawa, T.; Yuge, H. *J. Chem. Soc., Dalton Trans.* **1997**, 4127−4136.
(36) Decurtins, S.; Schmalle, H.; Pellaux, R. *New J. Chem.* **1998**, *22*, 117−121.
(37) Robson, R. In *Comprehensive Supramolecular Chemistry*, *Vol. 6*; Atwood, J. L., Davies, J. E. D., MacNicol, D. D., Vögtle, F., Lehn, J.-M., Eds.; Pergamon: Oxford, 1996; pp 733−755.
(38) Batten, S. R.; Robson, R. *Angew. Chem., Int. Ed.* **1998**, *37*, 1460−1494.
(39) Sozzuni, P.; Comotti, A.; Bracco, S.; Simonutti, R. *Angew. Chem., Int. Ed.* **2004**, *43*, 2792−2797.
(40) Sekiya, R.; Nishikiori, S. *Chem. Commun.* **2001**, 2612−2613.
(41) Sekiya, R.; Nishikiori, S. *Chem. Eur. J.* **2002**, *8*, 4803−4810.

Table 1. Summary of the 27 Crystalline Inclusion Compounds $[Ni(SCN)_2(isoH)_2]\cdot xG$ Synthesized

compd	guest	*x*	type[a]	compd	guest	*x*	type[a]	compd	guest	*x*	type[a]
1a	perylene	1/2[b]	I	**4a**	naphthalene	1/2[b]	C	**4j**	mesitylene	0.55[c]	C
1b	benz[*a*]anthracene	1/2[b]	I	**4b**	anthracene[40]	1/2[b]	C	**4k**	9-fluorenone Oxime	0.46[c]	C
1c	anthraquinone	1/2[b]	I	**4c**	phenanthrene	0.33[c]	C	**4l**	1,5-naphthalenediol	1/2[b]	C
2a	diphenylbutadiyne	1/2[b]	II	**4d**	naphthacene	0.45[c]	C	**5a**	chrysene	0.5[c]	?[d]
2b	thianthrene	1/2[b]	II	**4e**	fluorene	0.45[c]	C	**5b**	benzo[*a*]pyrene	0.5[c]	?[d]
2c	9,10-dihydroanthracene	1/2[b]	II	**4f**	biphenyl[41]	1/2[b]	C	**5c**	dibenz[*a*,*h*]anthracene	0.5[c]	?[d]
2d	azobenzene	1/2[b]	II	**4g**	*p*-terphenyl	0.45[c]	C	**5d**	stilbene	0.5[c]	?[d]
2e	phenyl benzoate	1/2[b]	II	**4h**	1,4-diethynylbenzene	1/2[b]	C	**5e**	diphenyl sulfide	0.5[c]	?[d]
3	triphenylene	1/3[b]	III	**4i**	styrene	0.5[c]	C	**5f**	pentacene	0.45[c]	?[d]

[a] Structure type classified on the basis of the difference in the stacking mode of the 2D host layer: I, Type I; II, Type II; III, Type III; C, Channel Type. [b] The number of guests determined by elemental analysis and X-ray structure determination. [c] The number of guests determined by elemental analysis (see text). [d] Structure type was not confirmed because of poor-crystal quality for X-ray structure determination.

Scheme 2. Chemical Structures of the 27 Guests Included in the Crystalline Host of $[Ni(SCN)_2(isoH)_2]_\infty$

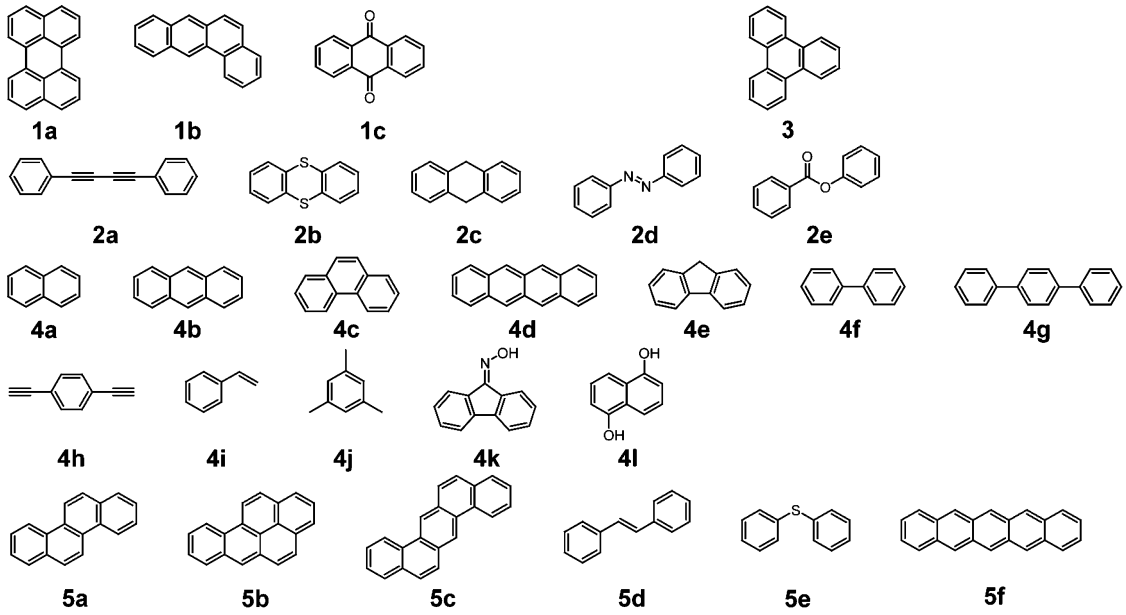

shape of the rectangular cavity implies that planar aromatic molecules would be included in it. The aim of the present study is to report the details of the inclusion ability of the crystalline host and to clarify the relationship between the molecular structure of the guest and the resultant 3D structure.

Synthesis

Crystalline inclusion compounds were obtained by slow evaporation at ambient temperature of acetonitrile solution containing Ni^{2+}, SCN^-, isoH, and a guest. Their IR spectra showed strong peaks at 2124 and 1707 cm^{-1}, characteristic of SCN^- and the carbonyl group of isoH, respectively, and a broad featureless absorption band in the range of 2300−3400 cm^{-1} which stems from hydrogen bonding of the isoH dimer. The crystals are insoluble in common organic solvents, except for polar ones such as DMF and DMSO. The guest in the crystal was confirmed by ^1H NMR (DMSO-d_6) measurement. The chemical formulas of the inclusion compounds were determined to be $[Ni(SCN)_2(isoH)_2]\cdot xG$, where G is a guest and the number of the guest $x = 0.33-0.66$ by elemental analysis and X-ray single-crystal crystallographic analysis.

Results and Discussions

General Features of the 2D Host Layer. A total of 27 crystalline inclusion compounds were successfully obtained from acetonitrile solution at ambient temperature. The guests included in the present host are summarized in Table 1, and their chemical structures are depicted in Scheme 2. Most of them are planar aromatic molecules, as expected as discussed above. The crystals of the inclusion compounds are generally dark green. In several cases, the crystals which include colored guests were brown for perylene (**1a**), azobenzene (**2d**), and 1,5-naphthalenediol (**4l**) inclusion compounds, orange for the naphthacene (**4d**) inclusion compound, and purple for the pentacene inclusion compound (**5f**). Of all the inclusion compounds, 21 were crystallized in diffraction quality. Their crystal structures were determined by single-crystal X-ray diffraction. The main crystallographic data are summarized in Table 2. All of the inclusion compounds examined here crystallized in the triclinic crystal system with space group $P\bar{1}$ (No. 2).

X-ray structure analysis revealed that the 21 inclusion compounds are constructed by stacking of identical 2D host layers with van der Waals contact separation. A ball-and-stick diagram of the host framework formed in the perylene inclusion compound (**1a**), with the atomic numbering scheme, is shown in Figure 1a, and its space-filling view is shown in Figure 1b. Both of them represent the host framework commonly formed in the other inclusion compounds. In the asymmetric unit, there are two symmetry-independent Ni^{2+} ions that sit on the inversion centers. Neighboring Ni^{2+} ions are doubly linked by two SCN^-

Table 2. Crystallographic Data for the Crystalline Inclusion Compounds of $[Ni(SCN)_2(isoH)_2]\cdot x$Guest

	1a	**1b**	**1c**	**2a**	**2b**	**2c**
formula	$C_{24}H_{16}N_4O_4S_2Ni$	$C_{23}H_{16}N_4O_4S_2Ni$	$C_{20}H_{14}N_4O_5S_2Ni$	$C_{44}H_{30}N_8O_8S_4Ni_2$	$C_{40}H_{28}N_8O_8S_6Ni_2$	$C_{42}H_{32}N_{10}O_8S_4Ni_2$
FW	547.2	535.2	525.2	1044.4	1058.6	1022.4
T (K)	293	293	293	293	293	293
crystal system	triclinic	triclinic	triclinic	triclinic	triclinic	triclinic
space group	$P\bar{1}$ (No. 2)	$P\bar{1}$ (No. 2)	$P\bar{1}$ (No. 2)	$P\bar{1}$ (No. 2)	$P\bar{1}$ (No. 2)	$P\bar{1}$ (No. 2)
a (Å)	9.6457(4)	10.025(2)	9.550(1)	14.6748(7)	14.4712(2)	14.8275(7)
b (Å)	10.9995(4)	11.0678(9)	11.0709(5)	11.0746(4)	11.0881(4)	11.0772(4)
c (Å)	18.0253(8)	17.963(2)	16.544(1)	18.0503(7)	16.6043(7)	16.523(1)
α (°)	116.502(2)	114.955(7)	101.862(5)	115.604(3)	103.158(3)	101.697(4)
β (°)	55.617(2)	50.81(2)	54.84(1)	70.413(3)	65.352(2)	64.114(5)
γ (°)	131.927(1)	131.83(1)	127.758(8)	77.837(2)	75.672(2)	74.884(3)
V (Å^3)	1166.8(2)	1151(3)	1101(2)	2263.6(8)	2174.3(5)	2194.9(9)
Z	2	2	2	2	2	2
ρ_{calcd} (g cm^{-3})	1.56	1.54	1.58	1.53	1.62	1.55
μ (mm^{-1})	1.050	1.063	1.113	1.079	1.217	1.111
$2\theta_{max}$ (°)	60	60	60	60	60	60
reflns obsd[a]	6664	5997	6123	12603	12116	11109
reflns used[b]	4419	3910	3904	6445	6956	5625
parameters	319	391	301	595	577	577
R1[c]	0.0569	0.0670	0.0630	0.0742	0.0731	0.0902
wR2[d]	0.1291	0.1772	0.1485	0.1703	0.1621	0.2045
GOF	1.117	1.096	1.146	1.034	1.093	1.096
$\Delta\rho_{max}$ (e Å^{-3})	+0.384	+0.394	+0.452	+0.506	+0.470	+0.484
$\Delta\rho_{min}$ (e Å^{-3})	−0.473	−0.867	−0.447	−0.499	−0.512	−0.516

	2d	**2e**	**3**	**4a**	**4b**
formula	$C_{40}H_{30}N_{10}O_8S_4Ni_2$	$C_{41}H_{30}N_8O_{10}S_4Ni_2$	$C_{60}H_{42}N_{12}O_{12}S_6Ni_3$	$C_{19}H_{14}N_4O_4S_2Ni$	$C_{21}H_{15}N_4O_4S_2Ni$
FW	1024.4	1040.4	1491.6	485.2	510.2
T (K)	293	293	293	293	293
crystal system	triclinic	triclinic	triclinic	triclinic	triclinic
space group	$P\bar{1}$ (No. 2)	$P\bar{1}$ (No. 2)	$P\bar{1}$ (No. 2)	$P\bar{1}$ (No. 2)	$P\bar{1}$ (No. 2)
a (Å)	14.517(1)	14.588(3)	17.8740(8)	7.2842(8)	7.2337(7)
b (Å)	11.1164(8)	11.100(2)	11.1970(5)	11.138(2)	11.013(1)
c (Å)	17.036(1)	17.026(3)	16.9305(7)	16.553(1)	16.727(2)
α (°)	105.706(5)	106.35(1)	103.836(3)	101.459(7)	104.590(3)
β (°)	64.698(6)	64.07(1)	78.041(4)	51.297(5)	54.736(5)
γ (°)	76.696(5)	77.091(5)	86.770(2)	100.017(6)	97.602(8)
V (Å^3)	2196(1)	2179.0(6)	3198.6(4)	1024.9(5)	1052.7(5)
Z	2	2	2	2	2
ρ_{calcd} (g cm^{-3})	1.55	1.59	1.55	1.57	1.61
μ (mm^{-1})	1.111	1.126	1.141	1.184	1.158
$2\theta_{max}$ (°)	60	60	60	60	55
reflns obsd[a]	11842	9304	15190	5832	4652
reflns used[b]	6853	5012	5524	4951	3772
parameters	705	722	511	249	292
R1[c]	0.0739	0.0878	0.1449	0.0370	0.0393
wR2[d]	0.1790	0.2175	0.3702	0.1092	0.1408
GOF	1.113	1.059	1.103	1.117	1.156
$\Delta\rho_{max}$ (e Å^{-3})	+0.534	+0.471	+0.851	+0.425	+0.513
$\Delta\rho_{min}$ (e Å^{-3})	−0.699	−1.394	−0.687	−0.560	−0.482

	4c	**4d**	**4e**	**4f**	**4g**
formula	$C_{18.62}H_{13.3}N_4O_4S_2Ni$	$C_{22.1}H_{15.4}N_4O_4S_2Ni$	$C_{19.85}H_{14.5}N_4O_4S_2Ni$	$C_{20}H_{15}N_4O_4S_2Ni$	$C_{22.1}H_{16.3}N_4O_4S_2Ni$
FW	478.7	522.7	497.7	498.1	523.7
T (K)	293	293	293	293	293
crystal system	triclinic	triclinic	triclinic	triclinic	triclinic
space group	$P\bar{1}$ (No. 2)	$P\bar{1}$ (No. 2)	$P\bar{1}$ (No. 2)	$P\bar{1}$ (No. 2)	$P\bar{1}$ (No. 2)
a (Å)	7.1699(8)	7.102(1)	7.5181(7)	7.5146(5)	7.2428(5)
b (Å)	11.1246(7)	11.068(2)	11.0616(8)	11.107(1)	11.0733(3)
c (Å)	16.440(1)	16.487(2)	16.806(1)	16.504(1)	16.4650(5)
α (°)	101.177(4)	100.256(8)	104.147(3)	102.267(4)	100.343(3)
β (°)	52.427(3)	51.497(8)	51.741(3)	52.054(3)	50.698(3)
γ (°)	100.679(6)	100.532(4)	98.910(6)	96.638(4)	100.469(2)
V (Å^3)	1015.8(3)	993.6(8)	1064.1(3)	1061.3(3)	1001.2(3)
Z	2	2	2	2	2
ρ_{calcd} (g cm^{-3})	1.56	1.75	1.55	1.56	1.74
μ (mm^{-1})	1.194	1.229	1.143	1.146	1.220
$2\theta_{max}$ (°)	60	60	60	60	60
reflns obsd[a]	5542	5634	5887	6026	5423
reflns used[b]	3323	4080	4102	4747	3905
parameters	229	229	229	283	229
R1[c]	0.1013	0.0753	0.1254	0.0387	0.0930
wR2[d]	0.3149	0.2834	0.4043	0.1103	0.3248
GOF	1.121	1.147	1.582	1.111	1.092
$\Delta\rho_{max}$ (e Å^{-3})	+1.802	+2.509	+4.541	+0.424	+2.758
$\Delta\rho_{min}$ (e Å^{-3})	−0.854	−0.899	−0.895	−0.451	−0.897

Table 2. (Continued)

	4h	4i	4j	4k	4l
formula	$C_{19}H_{13}N_4O_4S_2Ni$	$C_{18}H_{14}N_4O_4S_2Ni$	$C_{18.95}H_{16.6}N_4O_4S_2Ni$	$C_{19.98}H_{14.14}N_{4.46}O_{4.46}S_2Ni$	$C_{19}H_{14}N_4O_5S_2Ni$
FW	484.2	473.2	487.7	512.2	501.2
T (K)	293	293	293	293	293
crystal system	triclinic	triclinic	triclinic	triclinic	triclinic
space group	$P\bar{1}$ (No. 2)	$P\bar{1}$ (No. 2)	$P\bar{1}$ (No. 2)	$P\bar{1}$ (No. 2)	$P\bar{1}$ (No. 2)
a (Å)	7.1429(8)	7.1364(5)	7.1116(9)	7.704(1)	7.163(2)
b (Å)	11.115(1)	11.104(1)	11.137(1)	11.095(2)	11.161(3)
c (Å)	16.291(2)	16.489(1)	16.594(2)	16.481(2)	16.542(4)
α (°)	98.958(7)	100.589(4)	101.335(4)	100.924(7)	100.84(1)
β (°)	53.860(5)	51.940(3)	52.758(5)	52.79(1)	51.73(2)
γ (°)	99.271(4)	100.650(3)	101.198(8)	100.947(5)	101.08(1)
V (Å^3)	1027.9(5)	1006.9(3)	1021.1(5)	1006(1)	1015(2)
Z	2	2	2	2	2
ρ_{calcd} (g cm^{-3})	1.56	1.56	1.59	1.68	1.64
μ (mm^{-1})	1.181	1.203	1.189	1.114	1.203
$2\theta_{max}$ (°)	60	60	60	60	60
reflns obsd[a]	5411	5486	5169	5399	5397
reflns used[b]	3268	3485	4051	3464	2630
parameters	274	229	229	229	284
R1[c]	0.0721	0.0846	0.0731	0.1020	0.0768
wR2[d]	0.1894	0.2820	0.2564	0.3358	0.2530
GOF	1.089	1.114	1.109	1.076	1.012
$\Delta\rho_{max}$ (e Å^{-3})	+0.743	+2.044	+1.605	+2.907	+0.704
$\Delta\rho_{min}$ (e Å^{-3})	−1.146	−0.657	−1.124	−0.930	−0.771

[a] Number of observed reflections. [b] Number of reflections used in the structure determination. [c] $R1 = (\sum||F_o| - |F_c||)/\sum|F_o|$. [d] $wR2 = [\{\sum(w(F_o^2 - F_c^2)^2)\}/\sum(w(F_o^2)^2)]^{1/2}$.

ions in antiparallel fashion to form a one-dimensional (1D) chain running along the *b* axis. The interval distance between Ni^{2+} ions is 5.4998(4) Å. The remaining axial sites are coordinated by two pyridine nitrogen atoms of isoH. The bond lengths of Ni(1)−N(1), Ni(1)−S(2), and Ni(1)−N(11) are 2.041(3), 2.4883(8), and 2.131(3) Å, respectively, and those of Ni(2)−N(2), Ni(2)−S(1), and Ni(2)−N(21)_1 are 2.024(3), 2.5492(9), and 2.114(3) Å, respectively. Thus, the coordination geometry around each Ni^{2+} ion is elongated octahedron. This is identical with those observed usually for the related complexes.[45] The 1D chains are connected by the isoH dimer wall, which connects Ni^{2+} ions with a distance of 16.3305(8) Å. An ORTEP drawing of the isoH dimer wall, with the atomic numbering scheme, is shown in Figure 2a. Hydrogen bond distances of O(11)···O(21) and O(12)···O(22) are 2.646(5) and 2.597(5) Å, respectively. Since the carboxyl hydrogen atoms could not be located in difference maps, the hydrogen atoms were placed at calculated positions adjacent to the oxygen atom with the longer carbon-to-oxygen bond length. The dimer wall is slightly bent, with a dihedral angle of 15.1(2)° between the pyridine rings. This Ni^{2+}−isoH−isoH−Ni^{2+} linkage is running along the [012] axis, resulting in the formation of the two types of rectangular cavities with different widths (A and B, depicted in Figure 1a). The wide cavity (A-type) and the narrow cavity (B-type) are alternating. The maximum width of the A-type cavity is 7.474(5) Å between O(11) and O(22)_1, so that its dimension is 16.33 × 5.50(min)−7.47(max) Å^2. On the other hand, the minimum width of the B-type cavity is 3.731(5) Å between O(22)_1 and O(11)_2, so that its dimension is 16.33 × 3.73(min)−5.50(max) Å^2. The heights of the two cavities are equivalent to the width of pyridine ring of isoH. The 2D host layers with chemical formula $[Ni(SCN)_2(isoH)_2]_\infty$ spread parallel to the *bc* plane of the triclinic unit cell and are stacked with van der Waals contact separation to form the inclusion compound.

Figure 2b shows the front and side views of the perylene guest included in the A-type cavity. Since the size of the perylene guest is somewhat larger than that of the A-type cavity, the peripheral phenyl rings of the guest partly stick out of the cavity. The aromatic plane of the guest is nearly parallel to that of the isoH dimer wall, with dihedral angles of 4.4(2)° and 12.6(2)° toward the pyridine planes *A* and *B*, respectively. Weak $\pi-\pi$ interaction works between the guest and the isoH dimer wall, the shortest contact being 3.609(5) Å. It should be noted that the anisotropic thermal displacement factors of the constituent atoms of the guest are considerably larger than those of the host constituents. This probably means that the host−guest interaction is not so strong. Figure 1b shows that the B-type cavity is too narrow to include the guest.

As will be described below, the stacking mode of the 2D host layers is affected by the size and shape of the guest. The inclusion compounds are categorized into four stacking modes, i.e., Type I, Type II, Type III, and Channel Type, according to the difference in the stacking mode of the layers. A schematic representation of these four stacking modes is shown in Scheme 3. Since the layers are stacked with van der Waals contact separation, a void is formed between the A-type cavity and the neighboring layer. We defined this void as an interlayer region. In the first category, Type I is the case in which the 2D host layers are stacked with slipping and, as a result, the A-type cavities are isolated from each other (Scheme 3a). Type II and Type III are characterized by a double cavity and a triple cavity, respectively. The double cavity is formed by the combination of the two A-type cavities and the one interlayer region (Scheme 3b). Similarly, the triple cavity is formed by the combination of the three A-type cavities and the two interlayer regions (Scheme 3c). Channel Type is characterized by a channel

(42) Yang, G.; Zhu, H. G.; Liang, B. H.; Chen, X. M. *J. Chem. Soc., Dalton Trans.* **2001**, 580−585.
(43) Harada, J.; Ogawa, K.; Tomoda, S. *J. Am. Chem. Soc.* **1995**, *117*, 4476−4478.
(44) Harada, J.; Ogawa, K.; Tomoda, S. *Acta Crystallogr., Sect. B* **1997**, *53*, 662−672.
(45) Hollingsworth, M. D. In *Comprehensive Supramolecular Chemistry, Vol. 6*; Atwood, J. L., Davies, J. E. D., MacNicol, D. D., Vögtle, F., Lehn, J.-M., Eds.; Pergamon: Oxford, 1996; pp 177−237.

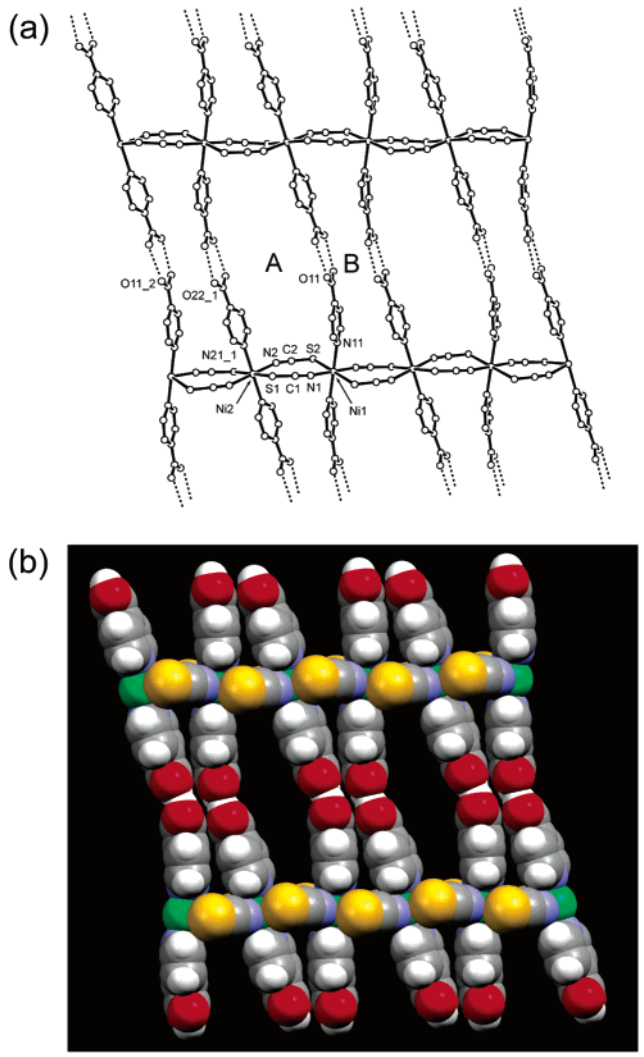

Figure 1. (a) View projected onto the *bc* plane of the host framework of $[Ni(SCN)_2(isoH)_2]_\infty$ formed in the perylene inclusion compound (**1a**). The wide (A) and narrow (B) rectangular cavities are arranged alternatingly in the *bc* plane. The perylene guests and hydrogen atoms are omitted for clarity. The broken lines show hydrogen bonds. _1 and _2 denote symmetry operations of $(-x, -y + 1, -z + 1)$ and $(x, y + 1, z)$, respectively. (b) Space-filling view of the host framework (white, hydrogen atom; gray, carbon atom; blue, nitrogen atom; red, oxygen atom; yellow, sulfur atom; green. nickel atom).

penetrating the stacked layers (Scheme 3d). **1a** belongs to Type I. Each category will be described in detail below.

In the following crystal structure descriptions, an axis setting common to all inclusion compounds is used for easy structural comparison among the compounds. The 1D chain and the Ni^{2+}−isoH−isoH−Ni^{2+} linkage run along the *b* axis and the [012] axis, respectively. The 2D host layers spread over the *bc* plane and are stacked along the *a* axis.

Type I. The following three guests form Type I inclusion compounds: perylene (**1a**), benz[*a*]anthracene (**1b**), and anthraquinone (**1c**). Their host−guest ratios are 1:0.5 (2:1) (a stoichiometric ratio of $[Ni(SCN)_2(isoH)_2]$ to a guest). As a representative example, the crystal structures of **1a** viewed along the *b* axis and the [012] axis are shown in Figure 3a and b, respectively. Figure 3a shows that the central moiety of the perylene guest is included in the A-type cavity (single cavity), while its peripheral moiety sticks out of it. Figure 3b shows that the layers are stacked along the *a* axis with slipping along the *b* axis by one-thirds of the *b* axis unit length. As a result of the slipping, the A-type cavity adjoins the B-type cavities of the neighboring layers, so that the A-type cavities are isolated from each other (Scheme 3a). These structural situations are also observed in **1b** and **1c**. Their crystal structures viewed along the *b* axis and the [012] axis are shown in Figures S1 and S2, respectively (Supporting Information).

Type II. Type II inclusion compounds are characterized by a bilayer structure in which the two A-type cavities and the one interlayer region are combined into the double cavity (Scheme 3b). The following five guests form Type II inclusion compounds: diphenylbutadiyne (**2a**), thianthrene (**2b**), 9,10-dihydroanthracene (**2c**), azobenzene (**2d**), and phenyl benzoate (**2e**). Although their host−guest ratios are 1:0.5 (2:1), these inclusion compounds are further classified into two categories according to the difference in the orientation of the guest relative to the isoH dimer wall. The one is represented by **2a** and the other by **2b**−**2e**.

The crystal structures of **2a** viewed along the *b* axis and the [012] axis are shown in Figure 4a and b, respectively. Figure 4a shows that the two diphenylbutadiyne guests related to each other by the inversion center span the two layers to afford the bilayer. This structural situation indicates that the two diphenylbutadiyne guests combine the two layers to form the bilayer structure. Although most parts of the guests are included in the double cavity, the peripheral phenyl rings partly stick out of it. Figure 4b shows that the resultant bilayers are stacked along the *a* axis with slipping along the *b* axis by one-third of the *b* axis unit length. In a manner similar to the A-type cavity of Type I, the double cavity adjoins the B-type cavities of the neighboring layers, so that the double cavities are isolated from each other.

In contrast to **2a**, the thianthrene guest (**2b**) and the 9,10-dihydroanthracene guest (**2c**) are oriented parallel to the isoH dimer wall. As a representative example, the crystal structures of **2b** viewed along the *b* axis and the [012] axis are shown in Figure 5a and Figure b, respectively. The packing situation shown in Figure 5a is reminiscent of Type I; nevertheless, thianthrene forms Type II. The reason for this is its molecular structure. Since thianthrene is a bent molecule, its convex part (sulfide groups) must be positioned at the widest region of the A-type cavity (Figure 6). Thus, its orientation is inevitably restricted to be parallel to the isoH dimer wall. Furthermore, thianthrene has a dipole moment stemming from its non-centrosymmetric molecular structure. In the double cavity, the neighboring guests are probably held together by dipole−dipole interaction and, as a result, the two layers are combined into the bilayer. It is well-known that this interaction is classified as a weak interaction, but recent statistical studies of molecular crystals revealed that even this type of weak interaction can affect the crystal structures of molecular crystals.[33] In a manner similar to **2a**, the thianthrene guests partly stick out of the double cavity. As a result, the bilayers are stacked with slipping to form Type II. These structural situations are also observed in **2c**. The crystal structures of **2c** viewed along the *b* axis and the [012] axis are shown in Figure S3.

It is interesting to note that the packing situations of the azobenzene guest (**2d**) and the phenyl benzoate guest (**2e**) are the same as those of the thianthrene guest and the 9,10-

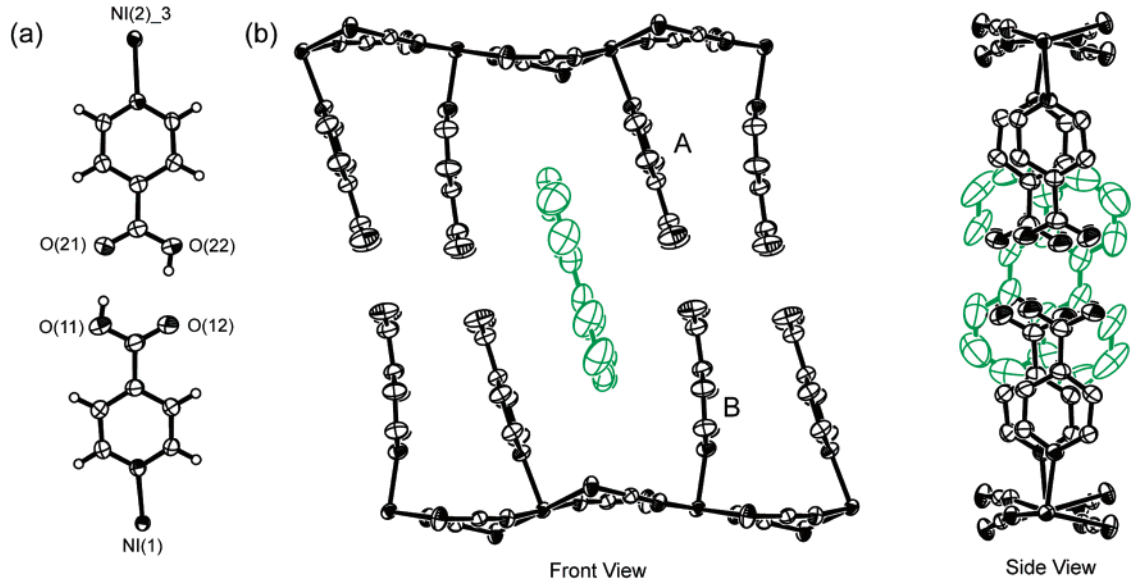

Figure 2. (a) ORTEP drawing of the isoH dimer wall formed in **1a**. _3 denotes symmetry operation of (x, y, $z + 1$). (b) ORTEP drawing of the front and side views of the perylene guest included in the A-type cavity. The perylene guest is nearly parallel to the isoH dimer wall. Hydrogen atoms are omitted for clarity.

Scheme 3. Schematic Representations of the Stacking Modes of Type I, Type II, Type III, and Channel Type[a]

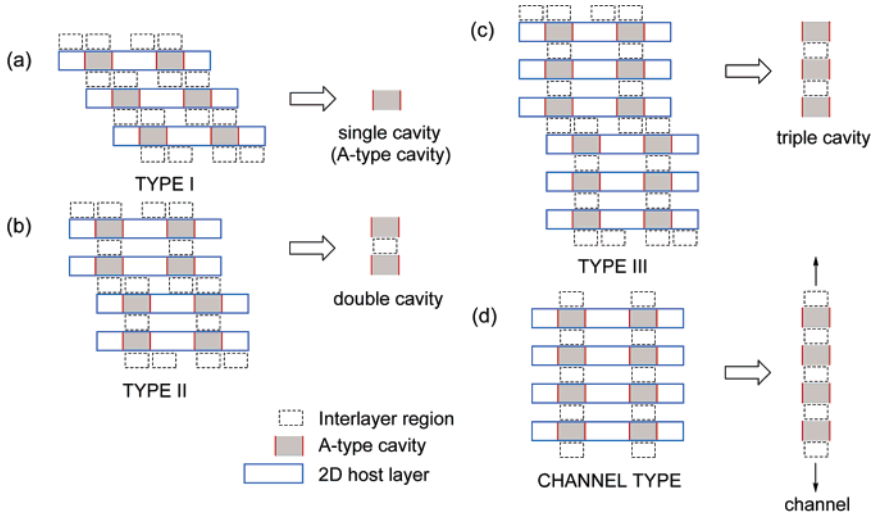

[a] The single cavity (top left) consists of one A-type cavity. The double cavity (bottom left) consists of two A-type cavities and one interlayer region. The triple cavity (top right) consists of three A-type cavities and two interlayer regions. The channel (bottom right) is formed by the one-dimensional array of A-type cavities and interlayer regions.

dihydroanthracene guest, although their molecular structures are quite different from those of the latter two molecules. As a representative example, the crystal structure of **2d** viewed along the *b* axis and the azobenzene guest included in the double cavity are shown in Figure 7a and b, respectively. Figure 7b shows that the azobenzene guests are disordered at two positions. Harada et al. have clarified that this type of disorder results from a pedal-like rotation of the azo group of azobenzene.[43,44] As a result of the pedal-like rotation, the central moiety of the azobenzene guest becomes thick compared to the peripheral phenyl rings and, in a manner similar to **2b**, its orientation is restricted to be parallel to the isoH dimer wall. Furthermore, the azobenzene guest is observed as a non-centrosymmetric molecule and, as a result, has dipole moment. In the double cavity, the two neighboring azobenzene guests are probably held together by dipole−dipole interaction. Thus, the two layers are combined into the bilayer. Since the azobenzene guests partly stick out of the double cavity (Figure 7a), the bilayer are stacked with slipping to form Type II. These structural situations are also observed in **2e**. The crystal structures of **2e** viewed along the *b* axis and the [012] axis are shown in Figure S4.

Type III. The Type III inclusion compound is characterized by a trilayer structure in which the three A-type cavities and the two interlayer regions are combined into the triple cavity (Scheme 3c). Only triphenylene (**3**) forms a Type III inclusion compound. The host−guest ratio is 1:0.33 (3:1). The crystal structures of **3** viewed along the *b* axis and the [012] axis are shown in Figure 8a and b, respectively. Figure 8a shows that the two triphenylene guests related to each other by the inversion center penetrate the three layers to afford the trilayer, where

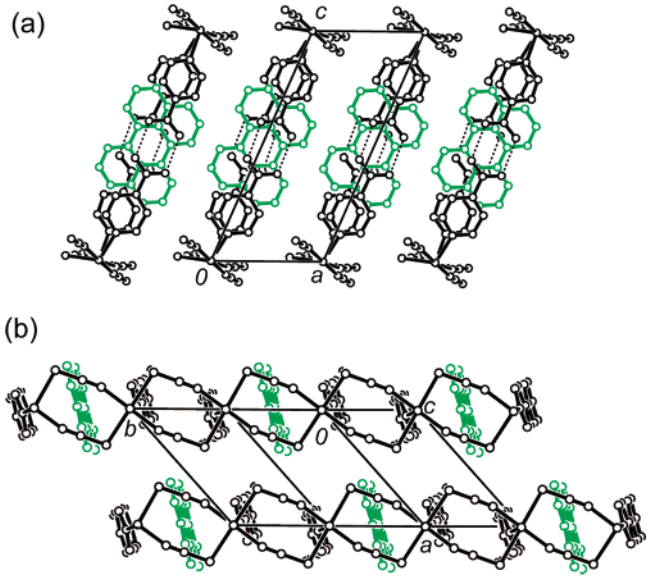

Figure 3. Crystal structures of the perylene inclusion compound (**1a**). (a) View along the *b* axis, which is the running direction of the 1D chain. The broken lines show hydrogen bonds. (b) View along the [0 1 2] axis, which is the running direction of the Ni^{2+}−isoH−isoH−Ni^{2+} linkage. The 2D host layers are stacked along the *a* axis with slipping along the *b* axis by one-third of the *b* axis unit length.

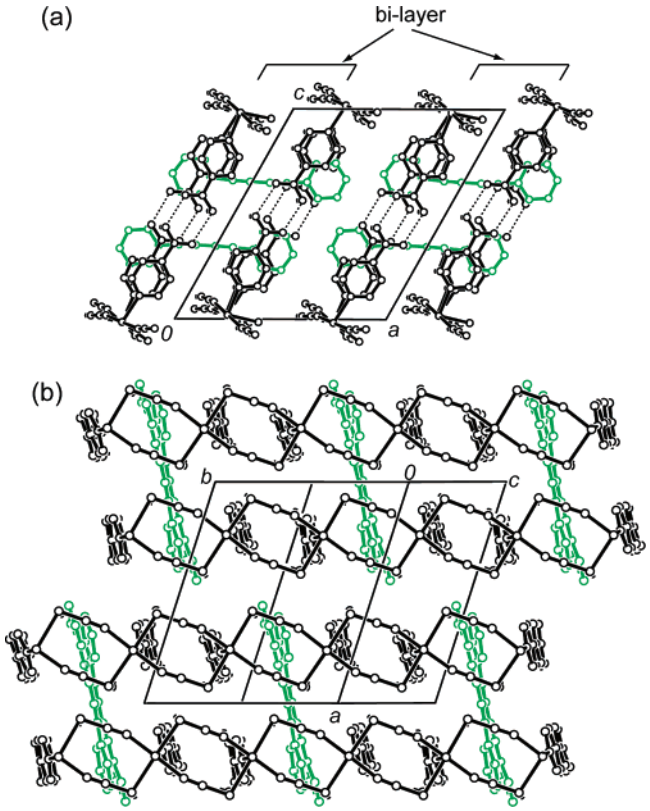

Figure 4. Crystal structures of the diphenylbutadiyne inclusion compound (**2a**). (a) View along the *b* axis. The broken lines show hydrogen bonds. (b) View along the [0 1 2] axis. The bilayers are stacked along the *a* axis with slipping along the *b* axis by one-third of the *b* axis unit length.

the A-type cavity of the central layer of the trilayer structure is shared equally by the two triphenylene guests. This structural situation indicates that the two triphenylene guests combine the three layers into the trilayer. Although most of the two triphenylene guests are included in the triple cavity, their

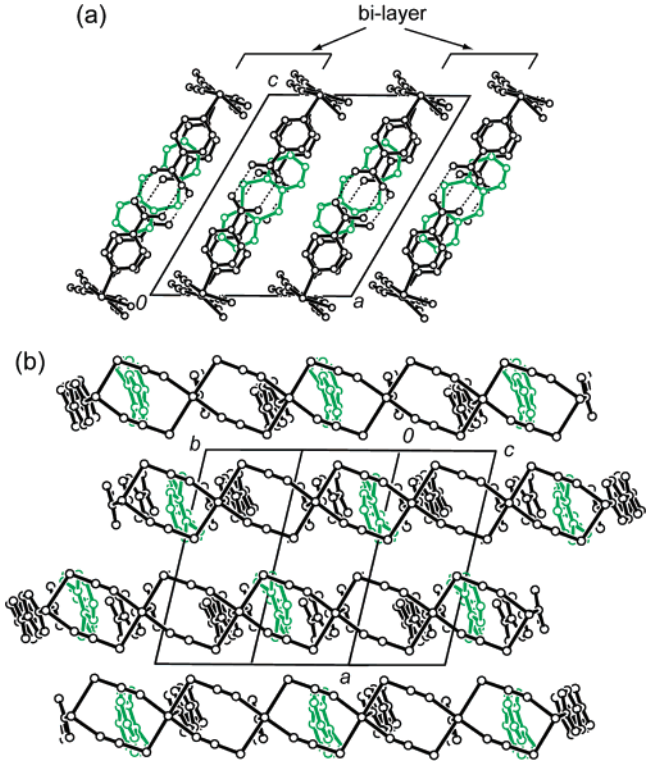

Figure 5. Crystal structures of the thianthrene inclusion compound (**2b**). (a) View along the *b* axis. The broken lines show hydrogen bonds. (b) View along the [012] axis.

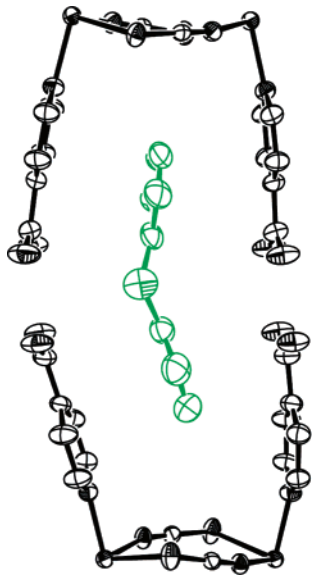

Figure 6. ORTEP drawing of the thianthrene guest included in the A-type cavity.

peripheral phenyl rings partly stick out of it. The resultant trilayers are stacked along the *a* axis with slipping along the *b* axis and the [012] axis. In a manner similar to the previous two stacking modes, the triple cavity adjoins the B-type cavities of the neighboring layers, so that the triple cavities are isolated from each other.

Channel Type. The structural feature of Channel Type has the channel penetrating the stacked 2D host layers (Scheme 3d). The following 12 guests (57% of the inclusion compounds obtained in diffraction quality) form Channel Type: naphthalene (**4a**), anthracene (**4b**),[40] phenathrene (**4c**), naphthacene (**4d**),

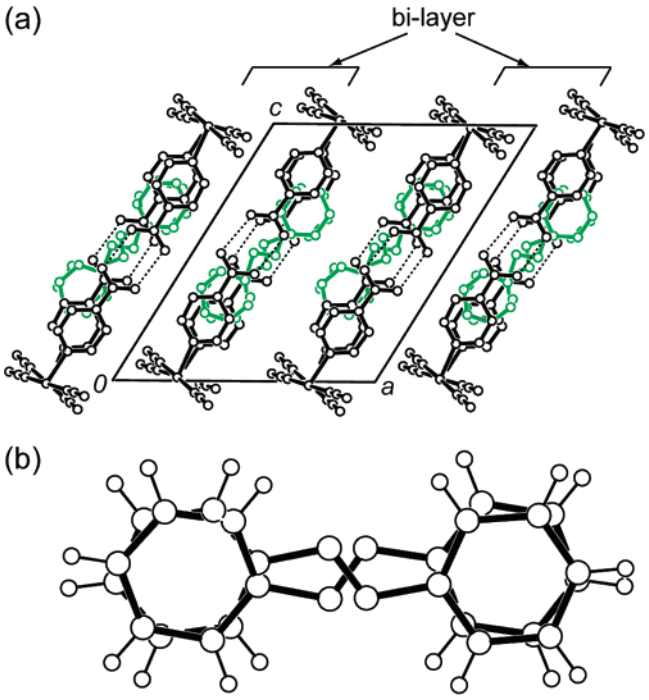

Figure 7. (a) Crystal structure of the azobenzene inclusion compound (**2d**) viewed along the *b* axis. The broken lines show hydrogen bonds. In the double cavity, each azobenzene guest is disordered at two positions. (b) Ball-and-stick representation of the azobenzene guest in the double cavity.

fluorine (**4e**), biphenyl (**4f**),[41] *p*-terphenyl (**4g**), 1,4-diethynylbenzene (**4h**), styrene (**4i**), mesitylene (**4j**), 9-fluorenone oxime (**4k**), and 1,5-naphthalenediol (**4l**). Among them, **4a**, **4b**, **4f**, **4h**, and **4l** form inclusion compounds with the host−guest ratios of 1:0.5 (2:1) while the others form incommensurate systems;[45] their host−guest ratios were estimated from elemental analysis. The crystal structure of **4l** is a representative example of Channel Type. Its views along the *b* axis and the [012] axis are shown in Figure 9a and b, respectively. In contrast to Types I−III, in Channel Type the layers are stacked along the *a* axis without slipping along the *b* axis. The A-type cavity is arranged one-dimensionally to form the channel penetrating the stacked layers, where the 1,5-naphthalenediol guests are arranged one-dimensionally. The O···O distance between the neighboring guests is 4.60(2) Å, indicating that there is no effective hydrogen bond between the guests. The 1,5-naphthalenediol guest is placed at the inversion center and spans the layers. This structural situation indicates that the 1,5-naphthalenediol guest combines the two layers. Therefore, it is evident that the one-dimensional array of the 1,5-naphthalenediol guests results in the formation of the channel. These structural situations are also observed in **4a**, **4b**, and **4f**. The crystal structures of **4a** viewed along the *b* axis and the [012] axis are shown in Figure S5.

In **4h**, the packing situation of the 1,4-diethynylbenzene guest is different from that in the previous four inclusion compounds. The crystal structure of **4h** viewed along the *b* axis is shown in Figure 10a. In contrast to the 1,5-naphthalenediol guest, the 1,4-diethynylbenzene guest is included *within* the A-type cavity; nevertheless, the 1,4-diethynylbenzene guest forms a Channel Type structure. This implies that a certain intermolecular interaction works between the neighboring guests as in the cases of **2b**−**2e**. The 1D array of the 1,4-diethynylbenzene guests is shown in Figure 10b. The distances of C(101)_1−H(101)_1···C(104) and C(101)_1−H(101)_1···C(105) are 3.015 and 3.216 Å, respectively. (The distances of C(101)_1···C(104) and C(101)_1···C(105) are 4.13(2) and 3.84(2) Å, respectively.) These facts indicate that the (phenyl) CH/π (ethynyl) interaction works between the neighboring 1,4-diethynylbenzene guests to form a 1D tape structure, leading to the formation of Channel Type.

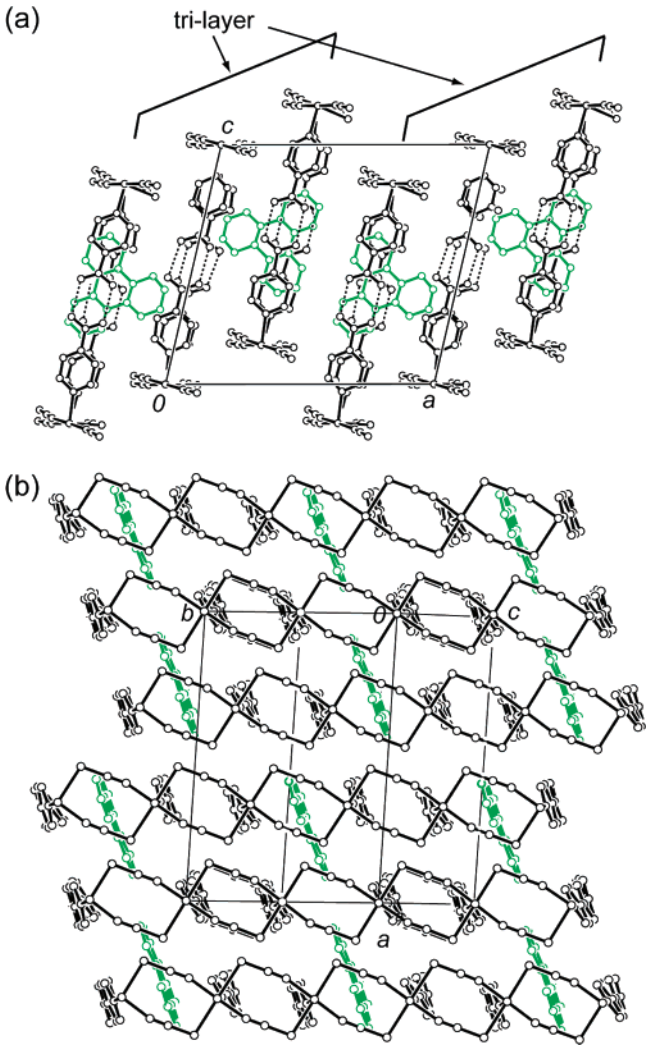

Figure 8. Crystal structures of the triphenylene inclusion compound (**3**). (a) View along the *b* axis. The broken lines show hydrogen bonds. (b) View along the [012] axis. The trilayers are stacked along the *a* axis with slipping along the *b* axis by one-third of the *b* axis unit length.

Interestingly, the other guests form the incommensurate inclusion compounds. Therefore, the spatial locations of the guests could not be determined by X-ray structure determination. This is because the crystallographic periodicities of the stacking of the layers are not coincident with those of the 1D array of the guests in the channels, although many peaks stem from the constituent atoms of the guests were found on their electron density maps. Table 1 shows that the host−guest ratios of the incommensurate system, which include linear molecules such as naphthacene (**4d**) and *p*-terphenyl (**4g**), are smaller, and the ratios of those systems which include small molecules such as mesitylene (**4j**) are larger than those of the commensurate systems[45] of 1:0.5. These tendencies can be rationally explained by the following: (1) the linear guests require larger space to be included in the channel compared to the guests that form

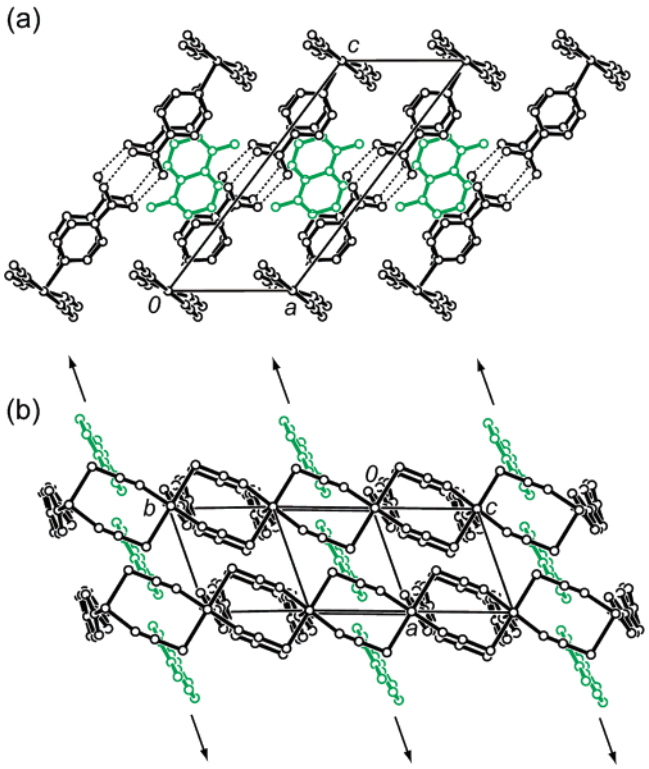

Figure 9. Crystal structures of the 1,5-naphthalenediol inclusion compound (**4l**). (a) View along the *b* axis. The broken lines show hydrogen bonds. (b) View along the [0 1 2] axis. The solid arrows denote the running direction of the channel.

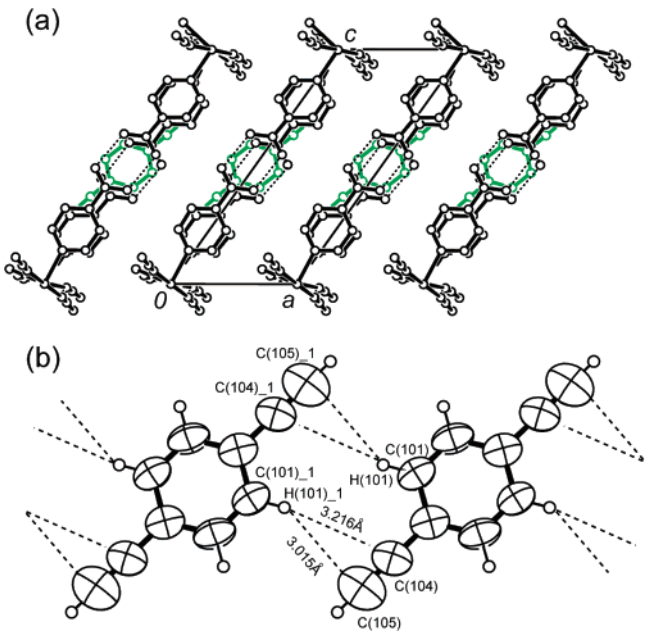

Figure 10. (a) Crystal structures of the 1,4-diethynylbenzene inclusion compound (**4h**) viewed along the *b* axis. The broken lines show hydrogen bonds. The 1,4-diethynylbenzene guest is included within the A-type cavity. (b) ORTEP drawing of the 1,4-diethynylbenzene guests arranged one-dimensionally in the channel. CH/π interaction works between the neighboring 1,4-diethynylbenzene guests to form the 1D type structure. _1 denotes symmetry operation of $(-x, -y + 1, -z + 1)$.

the commensurate system, so that their host−guest ratios become smaller than 0.5; (2) the small guests require smaller space to be included in the channel compared to the guests that form the commensurate system; furthermore, because of the close-packing requirement, the additional guests must be included in the channel, and thus, their host−guest ratios become larger than 0.5.

Other Inclusion Compounds and Limitations. In addition to the above 21 inclusion compounds, the following six crystalline inclusion compounds were also obtained: chrysene (**5a**), benzo[*a*]pyrene (**5b**), dibenz[*a*,*h*]anthracene (**5c**), stilbene (**5d**), diphenyl sulfide (**5e**), and pentacene (**5f**) inclusion compounds. As listed in Table 1, the host−guest ratios of **5a**−**5e** are 1:0.5, while that of **5f** is 1:0.45, which indicates that pentacene would form a Channel Type structure. Unfortunately, because they crystallized in low qualities, X-ray structure analysis could not be carried out. However, their IR spectra exhibited almost the same spectral patterns as those observed in **1**−**4**, except for the absorption peaks of the guests. These facts indicate that these inclusion compounds are constructed by stacking of the identical 2D host layers, and the above guests are included in the A-type cavities.

On the other hand, the present host cannot include aromatic bases (aniline, pyridine, etc.) and aromatic acids (benzoic acid and terephthalic acid). The reason for the former is that isoH is deprotonated by the bases. The reason for the latter may be that the aromatic acids hinder the isoH dimer formation by the formation of a carboxylic acid dimer between the aromatic acid and isoH.

As mentioned above, the present inclusion compounds are constructed by stacking of the identical 2D host layers. This means that the two-dimensional structure of the inclusion compound is predictable. Is it possible, then, to predict the 3D structure, in other words, the stacking mode of the layers? To answer this question, we should clarify the relationship between the molecular structure of the guest and the resultant stacking mode of the layers.

Mechanism of the Slipping. From the crystal structures of Types I−III, the slipping occurs when a guest partly sticks out of a discrete cavity (the discrete cavity denotes the A-type cavity for Type I, the double cavity for Type II, and the triple cavity for Type III). In Type I, the phenyl rings of the guests (**1a** and **1b**) or the carbonyl groups of the anthraquinone guest (**1c**) partly stick out of the A-type cavity, and as a result, the layers are stacked with slipping. In Type II, both sides of the phenyl rings of the diphenylbutadiyne guest (**2a**) or the phenyl rings of the guests (**2b**−**2e**) partly stick out of the double cavity to stack the bilayers with slipping. In Type III, the phenyl rings of the triphenylene guests partly stick out of the triple cavity. This made the trilayers stack with slipping. Thus, each discrete cavity adjoins the B-type cavities of the neighboring layers. The mechanism of this slipping can be rationally explained as follows: if the guests, the perylene guests for example, are arranged in a line (i.e., the layers are stacked without slipping and the A-type cavities are arranged in a line to form the channel as observed in Channel Type), steric hindrance would occur between the neighboring guests as shown in Scheme 4 (strictly speaking, steric hindarance occurs between hydrogen atoms of the perylene guest); alternatively, when convex parts (guests) of the layer adjoin the B-type cavities of the neighboring layer, the layer can engage well with the neighboring layer, affording a close-packed structure. Therefore, the slipping occurs when the guest partly sticks out of the discrete cavity to avoid steric repulsion and to form a close-packed structure.

Scheme 4

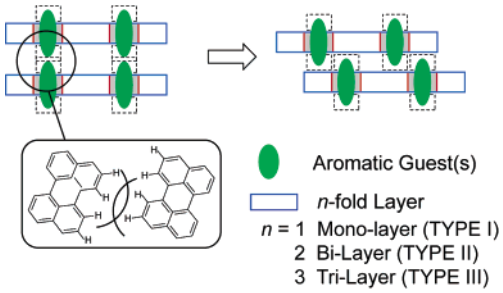

Relationship between Type *n* and Channel Type. On the other hand, the neighboring two layers are combined when the guest spans the layers (**2a** and **3**) or a certain intermolecular interaction works between the neighboring guests (**2b**−**2e**). Thus, it is anticipated that, for example, a guest which has length enough to penetrate a discrete cavity consisting of the four A-type cavities and the three interlayer regions and, simultaneously, has a suitable size and shape for filling this discrete cavity (i.e., the size of the guest is somewhat larger than that of the discrete cavity, as in the case of the perylene guest (**1a**)) would combine the four layers into a tetralayer. The resultant tetralayers would be stacked with slipping along the direction parallel to the 1D chain to form a Type IV structure. This means that the crystal structure of the present inclusion compound can be expressed in terms of an *n*-fold layer and the slipping. In the *n*-fold layer, the discrete cavity which consists of the *n* A-type cavities and the $(n - 1)$ interlayer regions are formed and the *m* guests are included in it. The *n*-fold layers are stacked with slipping to form Type *n*. It is thus clear that Channel Type is the case of Type ∞ (m, $n \rightarrow \infty$). In Channel Type, the layers are stacked without slipping, because the 1D array of the guests can be regarded as a molecule with infinite length.

Since a degree of the slipping is independent of the molecular structures of the guests and is almost constant, if we can clarify the relationship between the length of the discrete cavity and the number of guests included in it, the 3D structure of the inclusion compound can be predicted. The number of guests (m) included in the discrete cavity formed in the *n*-fold layer is closely related to the size and shape of the guest. When the guest has a suitable size and shape for filling this discrete cavity, the *m* guests that are required to fill it would be included in it to form Type *n*. Conversely, when a guest has an unsuitable size and shape for filling this discrete cavity, the guest would induce isomerization to another stacking mode, where a resultant discrete cavity can be filled with the guests. For example, triphenylene inevitably forms Type III because it has a suitable size and shape for filling the triple cavity ($n = 3$, $m = 2$). On the other hand, other stacking modes such as Type II and Type IV are unsuitable for triphenylene. If triphenylene forms Type II, the one molecule of triphenylene is included in the double cavity. (This is because the double cavity is too small to include the two molecules of triphenylene.) However, it cannot fill the double cavity, because its size is much smaller than that of the double cavity. Thus, triphenylene induces isomerization to Type III. Similarly, if triphenylene forms Type IV, the two molecules of triphenylene are included in the quadruple cavity. However, they cannot fill the quadruple cavity, because the size of the sum of the two guests is much smaller than that of the quadruple cavity. Thus, triphenylene induces isomerization to Type III.

Scheme 5

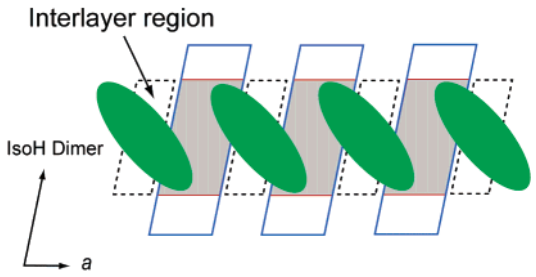

Type *n* or Channel Type? Whether a guest has a suitable size and shape for filling a discrete cavity is a curtail factor that determines whether the guest forms Type *n* or Channel Type. The guests compiled in Table 1 can be categorized into two types according to the resultant stacking modes. The one includes guests that have a suitable size and shape for filling a discrete cavity. Clearly this type of guest forms Type *n*. The other includes guests that cannot form close-packed structures because their size and shape are unsuitable for filling the discrete cavity. This type of guest forms Channel Type. The channel formation is structurally reasonable for the following reasons: (1) when the guest spans the layers and the guests are arranged one-dimensionally, the interlayer regions as well as the A-type cavities can be filled with the guests (Scheme 5); (2) the size of the channel is so large compared to any other discrete cavities that the guests can be efficiently included in it to form close-packed structures by adjusting the number of guests and their locations and orientations. Therefore, the guests categorized in the latter are arranged one-dimensionally to form Channel Type. Judging from the molecular structures of the guests that form Channel Type, small molecules and linear molecules tend to form Channel Type. This result also explains why 12 of the 21 guests form Channel Type. For the above reason, the conditions for the formation of Type *n* are much more severe than those for the formation of Channel Type. Thus, only a few guests can satisfy these conditions. Therefore, most of the guests form Channel Type.

Inclusion Ability. One of the striking features of the present host is its inclusion ability for a wide range of aromatic molecules. As shown in Scheme 2, this host can include aromatic molecules, from a small molecule such as mesitylene to large ones such as naphthacene, *p*-terphenyl, etc., by adapting the stacking mode to the molecular structure of the guest. For example, perylene forms Type I, diphenylbutadiyne forms Type II, triphenylene forms Type III, and 1,5-naphthalenediol forms Channel Type. Clearly, the size of the A-type cavity, with dimensions of ca. 16.3 Å × 5.5−7.5 Å^2, also plays an important role in the inclusion ability of the host. It is thus evident that the combination of the adaptability of the stacking mode to the molecular structure of the guest and the size of the A-type cavity produces the rich inclusion ability of the present host. On the basis of the results reported here, we anticipate that aromatic molecules within the size of the isoH dimer wall would be included in the A-type cavity to form Type *n* (n = I, II, III, ⋯, ∞).

The strong anisotropy of the crystal stems from the structural features and is also an important feature of the present inclusion compound. Because of the shape of the A-type cavity, any

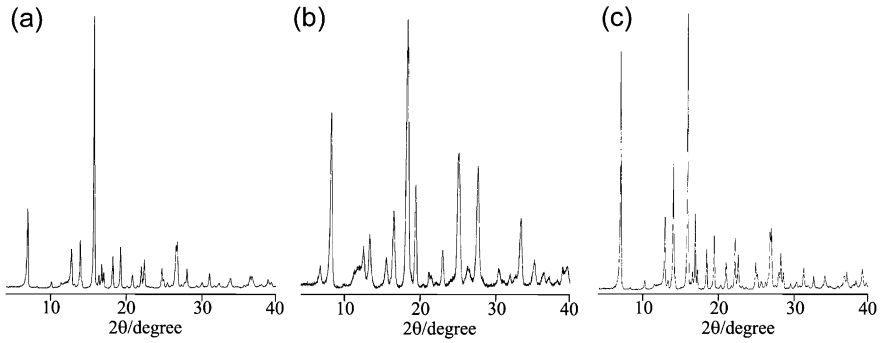

Figure 11. Powder X-ray diffraction patterns. (a) Naphthalene inclusion compound (**4a**). (b) Residual host (**4a-out**) obtained after the naphthalene guest was eliminated from **4a**. (c) Residual host after 24 h immersion into CH_2Cl_2 containing naphthalene at room temperature.

aromatic molecules included in it must orient their aromatic plane parallel to that of the isoH dimer wall. This strong anisotropy should be useful in developing materials of interest for their chemical and physical properties.[16]

Structural Robustness. The structural robustness of the host framework was investigated with X-ray powder diffraction (XRPD) and thermal gravimetric analysis (TGA). The naphthalene inclusion compound (**4a**) was used as a starting material for the following reasons: (1) **4a** has the channel penetrating the stacked layers, so the naphthalene guest should be released from the channels without collapsing the host framework; (2) the spatial location of the naphthalene guest in the channel is completely determined by X-ray structure analysis, which is required to simulate XRPD pattern; and (3) among **4a**, **4b**, **4f**, **4h**, and **4l**, the naphthalene guest is released from the channels at the lowest temperature.

TGA on **4a** (3.259 mg) showed two separate weight losses: an initial weight loss of 11% at 150 °C, corresponding to release of the naphthalene guest from the channels (13%, calculated), followed by another weight loss of 26% at 280 °C, corresponding to removal of HNCS (25%, calculated). The experimental evidence for the released species at each step includes the following: (1) upon heating of **4a** in a round-bottom flask at 120 °C in an oil bath, colorless crystals were formed on the inner surface of the flask; the ^{1}H NMR pattern of the colorless crystals in $CDCl_3$ was completely identical with that of naphthalene; (2) the IR spectrum of a light green powder obtained by heating **4a** over 280 °C showed two strong absorption peaks at 1610 and 1545 cm^{-1}, characteristic of isonicotinate (iso). On the other hand, those bands stemming from SCN^- ion and hydrogen bonding disappeared. This result indicates that the following decomposition occurs:

$$[Ni(isoH)_2(SCN)_2]_\infty \rightarrow [Ni(iso)_2]_\infty + 2HNCS\uparrow$$

Incidentally, XRPD of the residual light green powder showed significantly weak and broadened diffraction lines, indicating an amorphous state. **4a** was thus heated at 120 °C in vacuo, and a residual host (**4a-out**) was obtained. The diffraction patterns of **4a** and **4a-out** are shown in Figure 11a and b, respectively, and their IR spectra are also shown in Figure S6a and b, respectively. Comparison of the two diffraction patterns indicates that the crystal lattice of **4a** is changed to another one upon guest release. On the other hand, their IR spectra show that the location of each absorption peak, stemming from the host framework, remains unchanged. These facts indicate that the chemical environment of the 2D host layer is not changed at all. That is, at least the host framework should remain unchanged after release of the naphthalene guest from the channel. The change in XRPD patterns probably results from the slipping of the layers relative to the neighboring ones. We then investigated the reversibility of the inclusion process. **4a-out** was immersed into CH_2Cl_2 containing naphthalene for 24 h at room temperature. The diffraction pattern of the resultant sample is shown in Figure 11c, which is, without exception, identical with that of **4a**, serving as evidence of the reversibility. This result indirectly proves the robustness of the host framework.

Summary

In summary, we have successfully synthesized the novel crystalline inclusion compounds of $[Ni(SCN)_2(isoH)_2]\cdot xG$ (**1**−**5**), which are constructed through self-assembly of the host constituents (Ni^{2+}, SCN^-, and isoH) and aromatic guests. X-ray structure determination of the 21 inclusion compounds revealed that they are constructed by stacking of the identical 2D host layers with van der Waals contact separation. In the layer, the two types of rectangular cavities (the A-type and the B-type) are arranged alternatingly. The A-type cavity includes the aromatic guests of various sizes and shapes—from a small molecule such as mesitylene to large ones such as azobenzene, naphthacene, *p*-terphenyl, etc.—with their aromatic planes almost parallel to the isoH dimer wall, while the B-type cavity cannot include the guests due to its narrow width. The stacking mode of the layers is affected by the size and shape of the guest, and the 21 inclusion compounds were classified into four stacking modes, i.e., Type I, Type II, Type III, and Channel Type, according to the differences in the stacking modes of the layers. The former three stacking modes are characterized by their discrete cavities. The latter is characterized by the channel penetrating the stacked 2D host layers. The systematic investigation of the crystal structures of the 21 inclusion compounds clarified the close relationship between the molecular structure of the guest and the resultant stacking mode of the layers. This relationship indicates that the crystal structure of the present inclusion compound can be expressed in terms of the *n*-fold layer and the slipping. In the *n*-fold layer, the discrete cavity, which consists of the *n* A-type cavities and the $(n - 1)$ interlayer regions, is formed and *m* guests are included in it. This means that the present inclusion compound has a predictable 3D structure. From the viewpoint of the molecular recognition/inclusion event, the combination of the adaptability of the stacking mode to the molecular structure of the guest and the size of the A-type cavity with the dimension of ca. 16.5 Å ×

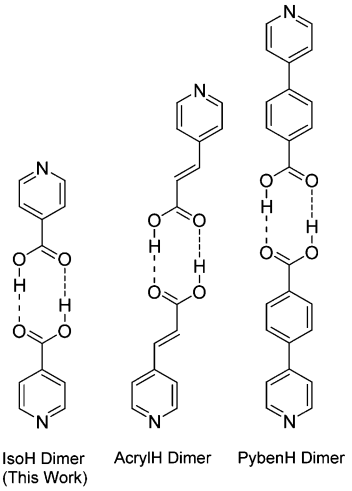

Figure 12. The isoH dimer wall (left), the 3-(4-pyridyl)propenoic acid (acrylH) dimer wall (center), and the 4-(4-pyridyl)benzoic acid (pybenH) dimer wall (right).

5.5−7.4 Å^2 produces the rich inclusion ability of the present host. XRPD and TGA indicated that the host framework remains unchanged after release of the guest and the residual host reversibly includes the guest.

Hitherto, hundreds of crystalline hosts have been designed and synthesized.[3] The molecular structures of host constituents have become increasingly complicated, which inevitably requires multistep synthetic procedures to synthesize the target hosts. In many cases, however, their inclusion abilities are still restricted to small organic molecules such as solvent molecules, benzene, naphthalene, and their analogues. Furthermore, prediction of the structure of a crystalline inclusion compound is still considerably difficult. However, we have overcome these difficulties by employing just two simple building blocks, isoH and SCN^- ion. The ability to predict the crystal structure and inclusion ability for a wide range of aromatic molecules would allow us to create compounds with intriguing physical and chemical properties in the future.

Future Remark 1: Extensible Host Framework

As shown in Scheme 1, the isoH dimer wall defines the dimension of the rectangular cavity, which means that its dimension can be expanded by exchanging the isoH dimer wall with longer building blocks. The resultant hosts should be able to include large aromatic molecules that cannot be included in the present host. Actually, by employing 3-(4-pyridyl)propenoic acid (acrylH)[41] and 4-(4-pyridyl)benzoic acid (pybenH) as building blocks (Figure 12), inclusion compounds that have much larger cavities have been successfully synthesized. Their crystal structures and inclusion abilities will be published elsewhere.

Future Remark 2: Magnetic Property of the 1D Chain Complex

It is important to note that there are few reports dealing with the magnetic property of Ni^{2+} ions connected one-dimensionally by SCN^- ions, although numerous attempts have been conducted to construct such systems.[46] The success in the construction of the 1D chain complex should be ascribed to the inherent flexibility of the isoH dimer wall. This is indirectly evidenced by the fact that replacement of the isoH dimer with other building blocks that consist of two or three components, such as the acrylH dimer,[41] an isoH−fumaricH_2−isoH "trimer",[41] and the pybenH dimer, do not affect the formation of the 1D chain complex. We are currently investigating the magnetic properties of the present inclusion compounds and trying to replace the Ni^{2+} ion with other transition metal ions, such as Fe^{2+}. The results will be published elsewhere.

Experimental Section

General Methods. All chemicals and solvents were purchased from Kanto Chemical Co., Ltd., Wako Pure Chemical Industries, Ltd., and Tokyo Kasei Kogyo Co., Ltd., and were used as received without further purification. ^{1}H NMR spectra of the inclusion compounds dissolved in DMSO-d_6 were recorded on a JEOL α-500 spectrometer with Larmor frequency of 500 MHz. All infrared (IR) spectra were measured on a JASCO FT/IR-350 spectrometer by KBr disk method at room temperature. Powder X-ray diffraction patterns were measured on a Rigaku Multi-Flex X-ray diffractometer using graphite-monochromated Cu Kα radiation (λ = 1.5418 Å) with a scanning rate of 1° min^{-1} at room temperature. Thermal gravimetric analysis (TGA) was carried out on a Seiko SSC-5200 at a scanning rate of 5° min^{-1} from 298 to 573 K with ca. 3.26 mg of the naphthalene inclusion compound (**4a**).

Synthesis. All inclusion compounds were prepared by the following method or a modification thereof. To acetonitrile (100 mL) in which $NiCl_2 \cdot 6H_2O$ (1.50 g, 6.3 mmol) was suspended, KSCN (1.52 g, 15.6 mmol) was added with vigorous stirring, and the mixture was refluxed for 1 h. After the precipitated KCl was filtered off, isonicotinic acid (1.61 g, 13.1 mmol) was dissolved. The solution was left for 24 h at room temperature, and then a guest was added. Crystals of the inclusion compound were obtained after slow evaporation of the solvent over a period of a few days at room temperature. The crystals were collected, washed with acetonitrile, and dried in the air. The compounds obtained were insoluble in common organic solvents, except for aprotic solvents such as DMF and DMSO. The presence of the guest was confirmed by ^{1}H NMR spectra of their DMSO-d_6 solutions, and the chemical formulas were determined by elemental analysis. The results of elemental analysis and some characteristic data are described below.

$[Ni(SCN)_2(isoH)_2]\cdot 0.5$(perylene) (**1a**): dark green, mp > 330 °C (dec); elemental analysis calcd for $C_{24}H_{16}N_4O_4S_2Ni$ (547.2), C 52.67, H 2.85, N 10.24, found C 52.87, H 2.82, N 10.27.

$[Ni(SCN)_2(isoH)_2]\cdot 0.5$(benz[*a*]anthracene) (**1b**): dark green, mp > 330 °C (dec); elemental analysis calcd for $C_{23}H_{16}N_4O_4S_2Ni$ (535.2), C 51.61, H 3.02, N 10.47, found C 51.59, H 3.06, N 10.39.

$[Ni(SCN)_2(isoH)_2]\cdot 0.5$(anthraquinone) (**1c**): dark green, mp > 330 °C (dec); elemental analysis calcd for $C_{20}H_{14}N_4O_5S_2Ni$ (525.2), C 48.02, H 2.69, N 10.66, found C 48.22, H 2.79, N 10.80.

$[Ni(SCN)_2(isoH)_2]\cdot 0.5$(diphenylbutadiyne) (**2a**): dark green, mp > 330 °C (dec); elemental analysis calcd for $C_{22}H_{15}N_4O_4S_2Ni$ (522.2), C 50.60, H 2.90, N 10.73, found C 50.68, H 2.89, N 10.65.

$[Ni(SCN)_2(isoH)_2]\cdot 0.5$(thianthrene) (**2b**): dark green, mp > 330 °C (dec); elemental analysis calcd for $C_{20}H_{14}N_4O_4S_3Ni$ (514.5), C 45.38, H 2.67, N 10.59, found C 45.73, H 2.76, N 10.42.

$[Ni(SCN)_2(isoH)_2]\cdot 0.5$(9,10-dihydroanthracene) (**2c**): dark green, mp > 330 °C (dec); elemental analysis calcd for $C_{26}H_{15}N_4O_4S_2Ni$ (511.2), C 49.33, H 3.16, N 10.96, found C 49.30, H 3.15, N 11.01.

$[Ni(SCN)_2(isoH)_2]\cdot 0.5$(azobenzene) (**2d**): dark green, mp > 330 °C (dec); elemental analysis calcd for $C_{20}H_{15}N_5O_4S_2Ni$ (512.2), C 46.89, H 2.96, N 13.68, found C 46.79, H 2.99, N 13.70.

$[Ni(SCN)_2(isoH)_2]\cdot 0.5$(phenyl benzoate) (**2e**): dark green, mp > 330 °C (dec); elemental analysis calcd for $C_{20.5}H_{15}N_4O_5S_2Ni$ (520.2), C 49.33, H 3.16, N 10.96, found C 49.30, H 3.15, N 11.01.

$[Ni(SCN)_2(isoH)_2]\cdot 0.33$(triphenylene) (**3**): dark green, mp > 330 °C (dec); elemental analysis calcd for $C_{22}H_{15}N_4O_4S_2Ni$ (522.2), C 48.31, H 2.81, N 11.27, found C 48.24, H 2.89, N 11.40.

(46) Maji, T. K.; Mostafa, G.; Clemente-Juan, J. M.; Ribas, J.; Lloret, F.; Okamoto, K.; Chaudhuri, N. R. *Eur. J. Inorg. Chem.* **2003**, 1005−1011.

$[Ni(SCN)_2(isoH)_2]$·0.5(naphthalene) (**4a**): dark green, mp > 330 °C (dec); elemental analysis calcd for $C_{19}H_{14}N_4O_4S_2Ni$ (480.1), C 47.03, H 2.91, N 11.55, found C 46.81, H 2.86, N 11.61.

$[Ni(SCN)_2(isoH)_2]$·0.5(anthracene) (**4b**):[40] dark green, mp > 330 °C (dec); elemental analysis calcd for $C_{21}H_{15}N_4O_4S_2Ni$ (510.2), C 49.43, H 2.97, N 10.98, found C 49.31, H 3.00, N 10.97.

$[Ni(SCN)_2(isoH)_2]$·0.33(phenanthrene) (**4c**): dark green, mp > 330 °C (dec); elemental analysis calcd for $C_{18.62}H_{13.3}N_4O_4S_2Ni$ (478.7), C 46.65, H 2.80, N 11.60, found C 46.74, H 32.88, N 11.60.

$[Ni(SCN)_2(isoH)_2]$·0.45(naphthacene) (**4d**): dark green, mp > 330 °C (dec); elemental analysis calcd for $C_{22.1}H_{15.4}N_4O_4S_2Ni$ (522.7), C 50.76, H 2.97, N 10.68, found C 51.03, H 2.99, N 10.12.

$[Ni(SCN)_2(isoH)_2]$·0.45(fluorene) (**4e**): dark green, mp > 330 °C (dec); elemental analysis calcd for $C_{19.85}H_{14.5}N_4O_4S_2Ni$ (497.7), C 48.14, H 2.96, N 11.28, found C 48.17, H 2.98, N 11.04.

$[Ni(SCN)_2(isoH)_2]$·0.5(biphenyl) (**4f**):[41] dark green, mp > 330 °C (dec); elemental analysis calcd for $C_{20}H_{15}N_4O_4S_2Ni$ (498.1), C 48.21, H 3.04, N 11.25, found C 48.04, H 3.04, N 11.31.

$[Ni(SCN)_2(isoH)_2]$·0.45(*p*-terphenyl) (**4g**): dark green, mp > 330 °C (dec); elemental analysis calcd for $C_{22.1}H_{16.3}N_4O_4S_2Ni$ (523.7), C 50.67, H 3.14, N 10.66, found C 50.55, H 3.10, N 10.55.

$[Ni(SCN)_2(isoH)_2]$·0.5(1,4-diethynylbenzene) (**4h**): dark green, mp > 330 °C (dec); elemental analysis calcd for $C_{19}H_{13}N_4O_4S_2Ni$ (484.2), C 47.13, H 2.71, N 11.57, found C 46.83, H 2.77, N 11.61.

$[Ni(SCN)_2(isoH)_2]$·0.5(styrene) (**4i**): dark green, mp > 330 °C (dec); elemental analysis calcd for $C_{18}H_{14}N_4O_4S_2Ni$ (473.2), C 45.69, H 2.99, N 11.84, found C 45.42, H 2.97, N 11.98.

$[Ni(SCN)_2(isoH)_2]$·0.55(mesithylene) (**4j**): dark green, mp > 330 °C (dec); elemental analysis calcd for $C_{18.95}H_{16.6}N_4O_4S_2Ni$ (487.7), C 46.66, H 3.43, N 11.52, found C 46.81, H 3.41, N 11.51.

$[Ni(SCN)_2(isoH)_2]$·0.46(9-fluorenone oxime) (**4k**): dark green, mp > 330 °C (dec); elemental analysis calcd for $C_{19.98}H_{14.14}N_{4.46}O_{4.46}S_2Ni$ (512.2), C 46.98, H 2.80, N 12.23, found C 47.04, H 2.71, N 12.16.

$[Ni(SCN)_2(isoH)_2]$·0.5(1,5-naphthalenediol) (**4l**): dark green, mp > 330 °C (dec); elemental analysis calcd for $C_{19}H_{14}N_4O_5S_2Ni$ (501.2), C 45.53, H 2.82, N 11.18, found C 45.43, H 2.84, N 11.09.

$[Ni(SCN)_2(isoH)_2]$·0.5(chrysene) (**5a**): dark green, mp > 330 °C (dec); elemental analysis calcd for $C_{23}H_{16}N_4O_4S_2Ni$ (535.2), C 51.61, H 3.02, N 10.47, found C 51.67, H 3.04, N 10.59.

$[Ni(SCN)_2(isoH)_2]$·0.5(benzo[*a*]pyrene) (**5b**): dark green, mp > 330 °C (dec); elemental analysis calcd for $C_{24}H_{16}N_4O_4S_2Ni$ (547.3), C 52.67, H 2.95, N 10.24, found C 52.64, H 3.03, N 10.31.

$[Ni(SCN)_2(isoH)_2]$·0.5(dibenz[*a*,*h*]anthracene) (**5c**): dark green, mp > 330 °C (dec); elemental analysis calcd for $C_{25}H_{17}N_4O_4S_2Ni$ (560.3), C 53.59, H 3.06, N 10.00, found C 53.43, H 3.09, N 10.05.

$[Ni(SCN)_2(isoH)_2]$·0.5(stilbene) (**5d**): dark green, mp > 330 °C (dec); elemental analysis calcd for $C_{21}H_{16}N_4O_4S_2Ni$ (511.2), C 49.33, H 3.16, N 10.96, found C 49.29, H 3.05, N 10.79.

$[Ni(SCN)_2(isoH)_2]$·0.5(diphenyl sulfide) (**5e**): dark green, mp > 330 °C (dec); elemental analysis calcd for $C_{20}H_{15}N_4O_4S_{2.5}Ni$ (514.3), C 46.71, H 2.95, N 10.90, found C 46.65, H 2.99, N 10.87.

$[Ni(SCN)_2(isoH)_2]$·0.45(pentacene) (**5f**): dark green, mp > 330 °C (dec); elemental analysis calcd for $C_{23.9}H_{16.3}N_4O_4S_2Ni$ (536.6), C 52.63, H 3.02, N 10.23, found C 52.89, H 2.81, N 10.32.

X-ray Crystal Structure Determinations. The intensity data were collected on a Rigaku RAXIS−RAPID imaging plate area detector using graphite-monochromatized Mo Kα radiation ($\lambda = 0.71069$ Å) at room temperature. The crystal structures were solved by the direct method using the SHELXS-97 program[47] and refined by successive differential Fourier syntheses and full-matrix least-squares procedure using the SHELXL-97 program.[48] Anisotropic thermal factors were applied to all non-hydrogen atoms. All hydrogen atoms were generated geometrically.

Crystal of **1a**: $C_{24}H_{16}N_4O_4S_2Ni$, FW = 547.2, triclinic, space group $P\bar{1}$ (No. 2), $a = 9.6457(4)$ Å, $b = 10.9995(4)$ Å, $c = 18.0253(8)$ Å, $\alpha = 116.502(2)°$, $\beta = 55.617(2)°$, $\gamma = 131.927(1)°$, $V = 1166.8(3)$ Å^3, $Z = 2$, μ(Mo Kα) = 1.184 mm^{-1}, $T = 293$ K. The intensity data collection was carried out for a 0.20 × 0.10 × 0.05 mm^3 size crystal in the range of $2.7° < 2\theta < 60.0°$ with ω scan. Empirical absorption correction was applied to 5832 reflections measured, and 4951 independent reflections ($F_o > 4\sigma(F_o)$) were used for the analysis. The final reliability factors were $R1(F_o) = 0.0569$, $wR2(F_o^2) = 0.1291$, and GOF = 1.117 for 319 parameters. The maximum and minimum electron density residues found in the final differential Fourier syntheses were +0.384 and −0.473 e Å^{-3}, respectively. The intensity data collection and structure analysis for the other crystals were carried out in a similar manner using the same diffractometer and programs, except for **2c**, whose crystal structure was solved by the direct method using the SIR-92 program.[49] In **4c**, **4d**, **4e**, **4g**, **4i**, **4j**, and **4k**, their guests were not included in the refinement calculations for the reason mentioned in the main text. Therefore, their final reliability factors had relatively large values. Crystallographic, experimental, and analytical data for the 21 compounds are listed in Table 2.

Acknowledgment. We are grateful to Professor Matsushita for permission to use the Rigaku RAXIS-RAPID imaging plate area detector. This work was supported by a Grant-in-Aid for Research-Fellowships of the Japan Society for the Promotion of Science for Young Scientists and Scientific Research (A) Project No. 12354008 from the Japan Society for the Promotion of Science.

Supporting Information Available: X-ray crystallographic files for the 21 inclusion compounds, in CIF format; crystal structures of **1b**, **1c**, **2c**, **2e**, and **4a**, and IR spectra of **4a** and **4a-out**. This material is available free of charge via the Internet at http://pubs.acs.org.

JA0463280

(47) Sheldrick, G. M. *SHELXS-97*, Program for the solution of crystal structures; University of Göttingen: Germany, 1997.
(48) Sheldrick, G. M. *SHELXL-97*, Program for the refinement of crystal structures; University of Göttingen: Germany, 1997.
(49) Altomare, A.; Burla, M. C.; Camalli, M.; Cascarano, G.; Giacovazzo, C.; Guagliardi, A.; Polidori, G. *SIR-92*, Program for the automatic solution of crystal structures; 1992.